






Cite this: *Chem. Commun.*, 2024, 60, 10768

Received 15th July 2024,  
Accepted 27th August 2024

DOI: 10.1039/d4cc03520h

rsc.li/chemcomm

## Polar organic cages for efficiently separating azeotropic mixtures†

Lukman O. Alimi, Xin Liu,  Gengwu Zhang, Basem Moosa  and Niveen M. Khashab  \*

**Dihydroxy-based polar organic cages (DIHO-cages) are reported to selectively separate toluene with 99.5% purity from an equimolar toluene/pyridine mixture, resulting in subsequent superior purification of pyridine. The efficient separation and purification, enhanced by strong and multiple host/guest C–H...O interactions between the cage and toluene, showcases DIHO-cages as a suitable candidate for the remarkable separation of such azeotropes on an industrial scale.**

One of the representative polar organic solvents that have been identified as “preferred” or “usable” industrial solvents is pyridine.<sup>1</sup> Pyridine with a boiling point of 115.3 °C is an important catalyst and solvent that is widely used in agrochemical, pharmaceutical and petrochemical industries.<sup>1</sup> Most importantly, the demand for pyridine globally is mostly driven by its increased pharmaceutical use and use as a denaturant in antifreeze mixtures.<sup>2</sup> On the other hand, toluene is heavily used to manufacture pesticides, coatings, synthetic resins, explosives, polyesters and benzoic acid.<sup>1</sup> Both toluene and pyridine are important industrial chemicals but pyridine often forms a minimum boiling binary azeotrope with toluene (boiling point 110.0 °C; pyridine/toluene 23 : 77, molar basis) during production, making separation of toluene from pyridine a difficult task; therefore, their purification has remained a great challenge.<sup>3,4</sup> Although several methods have been used with great success to separate and purify azeotropic mixtures, including azeotropic distillation,<sup>5</sup> pressure-swing distillation,<sup>6,7</sup> and extractive distillation<sup>8</sup> as well as other techniques, these methods have been bedevilled by high operating costs, high energy consumption and technical complexities.<sup>9</sup> So, the need for better and cost-effective methods is urgent and necessary. Some new separation strategies

that have emerged recently involve the use of the differences in the noncovalent interactions that exist between guests and crystalline nonporous adsorptive materials.<sup>10–17</sup> A few examples of these crystalline nonporous adsorptive materials have been reportedly used for separation of minimum-boiling binary azeotrope mixtures involving polar compounds such as pyridine.<sup>18–20</sup> The report by Chi and coworkers described the use of a new cavity-extended version of calix[4]pyrrole (C4P) that forms nonporous adaptive crystals for the effective separation of polar compounds from pyridine/toluene and 1,4-dioxane/water azeotrope mixtures.<sup>18</sup> In another study by Huang and coworkers, nonporous adaptive crystals of cucurbit[6]uril (Q[6]) could, by forming a host/guest complex, separate pyridine from a toluene/pyridine mixture with 100% purity.<sup>19</sup> Also, Isaacs and coworkers reported the separation of pyridine from azeotrope mixtures of toluene, benzene and pyridine with more than 99.9% purity even in a system with low pyridine content by using double-cavity nor-seco-cucurbit[10]uril (ns-Q[10]).<sup>20a</sup> Most recently, Li and coworkers reported the use of macrocycle cocrystals for efficient removal of pyridine from an equimolar toluene/pyridine mixture with 99.2% purity.<sup>20b</sup> Common to all these examples is that the separation occurs using the intrinsic cavity<sup>18,19,20a</sup> of specific dimensions as revealed by the crystal structures of their respective macrocycles and that these cavities could only capture the smaller-sized pyridine.

As part of the ongoing work in our group in the quest for organic cages showing excellent separation performances/applications, we have prepared and deployed a polar **DIHO-cage** endowed with hydrogen-bond-donor hydroxyl (–OH) groups and the possibility of forming extrinsic pores in their crystal packing that can accommodate any of these mixtures for efficient separation, in contrast to the case for macrocycles with fixed/pre-sized cavities. We have also recently established that a pre-sized or fixed cavity dimension is not a prerequisite for excellent separation, most especially when larger guest molecules are involved.<sup>21</sup> Herein, we utilized the polar organic **DIHO-cage** as adsorptive materials to separate an equimolar mixture of toluene/pyridine. Surprisingly, **DIHO-cage** can capture and separate **Tol** from an equimolar **Tol/Py** mixture with

Smart Hybrid Materials Laboratory (SHMs), Physical Science and Engineering, King Abdullah University of Science and Technology (KAUST), Thuwal, 23955-6900, Saudi Arabia. E-mail: niveen.khashab@kaust.edu.sa

† Electronic supplementary information (ESI) available: Experimental section and supporting figures, tables and crystallographic data. CCDC 2361427–2361431. For ESI and crystallographic data in CIF or other electronic format see DOI: <https://doi.org/10.1039/d4cc03520h>





**Scheme 1** Schematic representation of **DIHO-cage** as an adsorptive material for separation of toluene from pyridine in an equimolar mixture.

99.5% purity unlike most of the reported cases where pyridine is captured<sup>18–20</sup> instead of toluene (Scheme 1). To the best of our knowledge this is the first example of using a polar organic cage for efficient selective separation of **Tol** and subsequent purification of the polar compound **Py** from a **Tol/Py** binary mixture.

**DIHO-cage** was synthesized, with a good 70% yield, by carrying out a simple, cost-effective and one-step condensation reaction of 2,5-dihydroxyterephthalaldehyde with flexible tris(2-aminoethyl)amine (TREN) in acetonitrile (Scheme S1, ESI†).<sup>22</sup> Proton, <sup>13</sup>C NMR and mass spectra confirmed the successful synthesis of **DIHO-cage** (Fig. S1 and S2, ESI†). We chose **DIHO-cage** as our adsorbent as mentioned earlier because of its polar nature that would not only promote host/guest hydrogen bonding but also boost crystallinity.<sup>23</sup> Two different types of suitable single crystals of **DIHO-cage**, denoted as **DIHO-cage@DCM** and **DIHO-cage@CHCl<sub>3</sub>**, were obtained by diffusing acetonitrile into, respectively, DCM and chloroform solutions of **DIHO-cage** (Fig. S3 and Table S1, ESI†). **DIHO-cage@DCM** was observed to crystallize in the monoclinic system, specifically with the space group *P2<sub>1</sub>/c*, and **DIHO-cage@CHCl<sub>3</sub>** also crystallized in monoclinic system, but with the space group *C2/c*. Analysis of the crystal structures of **DIHO-cage** with DCM and chloroform revealed a high propensity for **DIHO-cage** to form complexes with most organic solvents utilizing the extrinsic pores in the crystal packing of the cage, like some other reported (2+3) organic cages (Fig. S1, ESI†).<sup>22,24–27</sup> In fact, inspection of the crystal structure of **DIHO-cage@DCM** showed two guest molecules of DCM with one molecule of the cage in the asymmetric unit, while inspection of the **DIHO-cage@CHCl<sub>3</sub>** crystal structure showed one molecule of the cage with one molecule of chloroform in the asymmetric unit (Fig. S3, ESI†).

Thermogravimetric analysis (TGA) of the as-synthesized **DIHO-cage** showed no appreciable weight loss as the temperature was increased up to 300 °C, indicating that it had no solvent left after being synthesized. Despite this lack of residual solvent in the as-synthesized cage, we decided to activate it at 40 °C for 2 h to ensure that it remained empty before use for all the subsequent experiments (Fig. S4, ESI†). Powder X-ray diffraction (PXRD) confirmed the bulk purity of the as-synthesized **DIHO-cage**. The PXRD pattern of the activated **DIHO-cage** confirmed that its crystallinity was retained after it was subjected to the desolvation procedure (Fig. S5, ESI†). The Brunauer–Emmett–Teller (BET) surface area of the

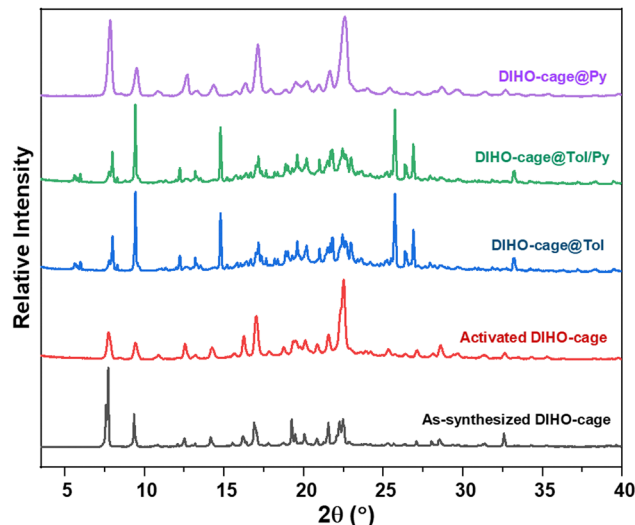


**Fig. 1** PXRD patterns showing the adsorption of **Tol** and **Py** by the **DIHO-cage** after 24 h exposure.

activated **DIHO-cage** was determined to be 14 m<sup>2</sup> g<sup>−1</sup> according to the N<sub>2</sub> gas sorption isotherm at 77 K, indicative of **DIHO-cage** being non-porous (Fig. S6, ESI†). The adsorption efficiency of the activated **DIHO-cage** in the presence of a mixture of pyridine and toluene was then tested by performing solid-vapour adsorption experiments. Notably, PXRD and <sup>1</sup>H-NMR results for single-component and 1:1 (v/v) binary mixture experiments indicated that **DIHO-cage** may be selective for toluene over pyridine (Fig. 1 and Fig. S7, ESI†).

The adsorption performance of **DIHO-cage** was further investigated using different ratios of **Tol** to **Py** (1:3 and 3:1 (v/v)) to replicate the ideal industrial situation and further understand the influence of these ratios on the **DIHO-cage** performance. The results of <sup>1</sup>H-NMR and gas chromatographic analyses of **DIHO-cage** samples exposed to these different ratios of toluene to pyridine confirmed a selective adsorption of toluene over pyridine with relatively high purity levels of 97.4% and 99.9% for, respectively, 1:3 and 3:1 (v/v) **Tol/Py** mixtures after one adsorption process (Fig. S8 and S9, ESI†). To investigate the dynamics of the adsorption process, we carried out time-dependent solid-vapour sorption experiments. It took **DIHO-cage** about 10 h to accommodate on average ca. 1.0 mole of **Tol** per cage, with an adsorption capacity of 134.9 mg g<sup>−1</sup> (Fig. S10, ESI†). To better understand the mechanism of the selective adsorption of **Tol** over **Py**, first single crystals of **DIHO-cage@Tol** were grown by effecting vapour diffusion of MeCN into a toluene/DCM solution of **DIHO-cage** at room temperature (Table S1, ESI†). Single crystals of **DIHO-cage@Py** were also obtained using the same approach with **Py**. Inspection of the crystal structure of **DIHO-cage@Tol** showed a 1:1 ratio of **DIHO-cage** to **Tol** (Fig. S11, ESI†).

In the crystal structure, the **Tol** guest molecules were situated, as expected, in the extrinsic cavity generated by the crystal packing (Fig. 2 and Fig. S12, ESI†). Inspection of the crystal packing of **DIHO-cage@Tol** showed **Tol** molecules situated



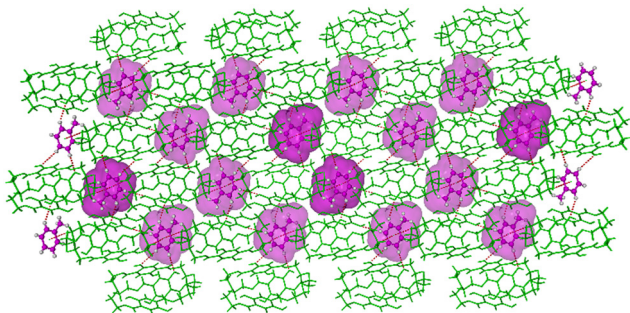


Fig. 2 Perspective view showing Tol guest molecules (pink) in the crystal packing of DIHO-cage@Tol.

between the two layers and forming a continuous channel when viewed along *b*-axis (Fig. S12, ESI†). Inspection of the crystal structure also showed multiple C–H...O host/guest intermolecular interactions, including those with lengths of 3.434 Å, 3.497 Å and 3.756 Å occurring between some of the protons on the Tol molecule and the oxygen atom of the –OH group on the cage molecule (Fig. 3 and Fig. S13 and Table S2, ESI†). The crystal packing also showed other noncovalent intermolecular interactions (e.g., C–H... $\pi$  = 3.703 Å, etc.) between some of the protons of the cage and the centroid of the aromatic ring of the Tol guest (Fig. 3).

Some host/host intermolecular interactions between two neighbouring cages also formed (Fig. S14 and Table S3, ESI†). Unlike the case for DIHO-cage@Tol, no Py guest molecule was found in the crystal structure of DIHO-cage@Py. The ability of DIHO-cage to form a complex with only Tol suggested its bias to favour the uptake of Tol from a Tol/Py mixture.

Furthermore, in all of the crystal structures available, very strong O–H...N intramolecular hydrogen bonding interactions formed within the cage (Fig. S15, ESI†). These strong intramolecular interactions, apart from preventing the aromatic groups from rotating, would appear to also outcompete any possibly formed intermolecular interactions, rendering the hydrogen atom on the –OH groups unavailable as an H-bond donor for intermolecular host–guest hydrogen bonding

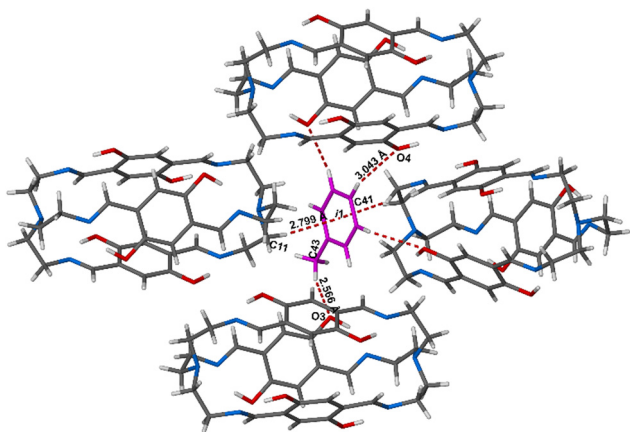


Fig. 3 Crystal packing showing various host–guest intermolecular interactions in DIHO-cage@Tol.

interactions, perhaps explaining why Py (H-bond acceptor) was not observed to have been captured by DIHO-cage.<sup>28</sup> Having established the ability of the Tol guest molecule to interact with DIHO-cage, it is important to mention that the size and/or shape of Tol could have also contributed to this selective uptake. DIHO-cage using its extrinsic cavity for the uptake implies no limitation on the cavity size or dimensions, therefore allowing for the most favorable orientations with the larger Tol guest molecule and not the smaller-sized Py to form stable host–guest intermolecular interactions.<sup>21,29</sup>

To further show the selectivity of DIHO-cage for Tol, we grew a single crystal in a 1 : 1 (v/v) mixture of toluene and pyridine. The orange single crystal obtained was analyzed using SCXRD and showed the same space group as that for the crystal obtained directly from toluene alone. This result confirmed the ability of DIHO-cage to selectively capture Tol from a Tol/Py mixture, a feature that can also be visualized due to the different colours of the crystals with/without Tol (Fig. 4 and Fig. S16–S18 and Table S1, ESI†). We then confirmed that the guest-free DIHO-cage can be regenerated from DIHO-cage@Tol simply by washing DIHO-cage@Tol with hexane and allowing it to dry at a very reduced temperature of 45 °C under vacuum. This approach ensured the robustness of the DIHO-cage, allowing it to withstand several adsorption–desorption processes/cycles while retaining its performance (Fig. S19 and 20, ESI†).

To further establish and corroborate the affinity of the DIHO-cage for Tol, a gas chromatography (GC) analysis was carried out. The results confirmed the adsorption and selectivity of Tol over Py by DIHO-cage with 99.5% purity (Fig. 5a and b) in one adsorption cycle. This high 99.5% purity of captured Tol persisted through five cycles of adsorption, and the purity of the Py left behind improved to ca. 100% (Fig. 5c and Fig. S21, ESI†). This observation further confirmed that obtaining highly pure Py could also be achieved.

In summary, we have successfully demonstrated that a polar crystalline organic cage (DIHO-cage) can selectively adsorb only toluene in 1 : 1, 1 : 3 and 3 : 1 (v/v) Tol/Py binary mixtures. DIHO-cage was found in this work to show a pair of advantages: efficient Tol uptake (99.5%) and subsequent superior purification of pyridine after a few cycles of adsorption. Despite DIHO-cage having the hydrogen donor hydroxyl group (–OH), it could only act as a hydrogen bond acceptor to form a host–guest

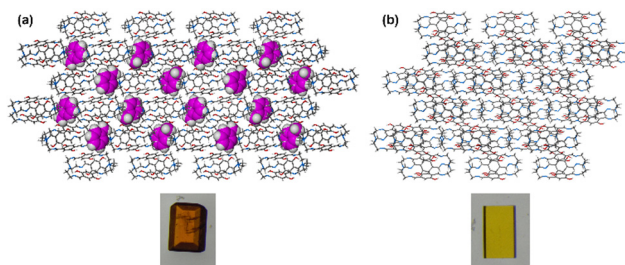


Fig. 4 Crystal packing and images of (a) DIHO-cage@Tol and (b) empty DIHO-cage@Py showing the vapochromic behaviour of DIHO-cage.







Fig. 5 (a) Relative amounts of **Tol** and **Py** adsorbed by activated DIHO-cage. (b) Percentages of **Tol** and **Py** adsorbed by activated DIHO-cage as determined using GC-MS. (c) Relative uptakes of **Tol** and **Py** after each of 5 adsorption processes/cycles.

complex with toluene (H-bond donor) instead of pyridine (H-bond acceptor) *via* numerous host/guest C–H...O and C–H... $\pi$  intermolecular interactions as revealed by their crystal structures. This interesting phenomenon endows **DIHO-cage** with an ability not displayed by some recently reported adsorptive materials, namely to capture only toluene from a Tol/Py azeotrope mixture. This selective uptake and subsequent purification are accompanied with a color change, enabling the direct visualization of the entire adsorption of **Tol** by **DIHO-cage**. We believe that this result would serve as an excellent precedent for more remarkable separations of other azeotrope mixtures using organic cages.

All authors have given approval to the final version of the manuscript.

We thank KAUST for supporting this work.

## Data availability

The data supporting this article have been included as part of the ESI† with the crystallographic data for all the structures deposited at the CCDC and accessible at <https://www.ccdc.cam.ac.uk/structures>.

## Conflicts of interest

There are no conflicts to declare.

## Notes and references

- G. Modla, *Energy*, 2013, **50**, 103–109.

- Pyridine Market Size by Type, Regions, Global Industry Analysis, Share, Growth, Trends, and Forecast 2024 to 2033, <https://www.thebrainyinsights.com/report/pyridine-market-14125>.
- C. H. Schneider and C. C. Lynch, *J. Am. Chem. Soc.*, 1943, **65**, 1063.
- D. R. Lide, *CRC Handbook of Chemistry and Physics*, CRC Press, Boca Raton, FL, 2005, pp. 6–194. Internet version: <https://www.hbcpnetbase.com>, accessed 2021-10-30.
- M. Errico, B.-G. Rong, G. Tola and M. Spano, *Ind. Eng. Chem. Res.*, 2013, **52**, 1612–1619.
- W. L. Luyben, *Chem. Eng. Process.*, 2018, **123**, 174–184.
- S. Liang, Y. Cao, X. Liu, X. Li, Y. Zhao, Y. Wang and Y. Wang, *Chem. Eng. Res. Des.*, 2017, **117**, 318–335.
- Y. Wang, X. Zhang, X. Liu, W. Bai, Z. Zhu, Y. Wang and J. Gao, *Sep. Purif. Technol.*, 2018, **191**, 8–26.
- J. Qi, Y. Li, J. Xue, R. Qiao, Z. Zhang and Q. Li, *Sep. Purif. Technol.*, 2020, **238**, 116487.
- J. R. Wu and Y. W. Yang, *Angew. Chem., Int. Ed.*, 2021, **60**, 1690–1701.
- K. C. Jie, Y. J. Zhou, E. R. Li and F. Huang, *Acc. Chem. Res.*, 2018, **51**, 2064–2072.
- A. Dey, S. Chand, B. Maity, P. M. Bhatt, M. Ghosh, L. Cavallo, M. Eddaoudi and N. M. Khashab, *J. Am. Chem. Soc.*, 2021, **143**, 4090–4094.
- H. Yao, Y. M. Wang, M. Quan, M. U. Farooq, L. P. Yang and W. Jiang, *Angew. Chem., Int. Ed.*, 2020, **59**, 19945–19950.
- A. Dey, S. Chand, M. Ghosh, M. Altamimy, B. Maity, P. M. Bhatt, I. A. Bhat, L. Cavallo, M. Eddaoudi and N. M. Khashab, *Chem. Commun.*, 2021, **57**, 9124–9127.
- B. Hua, Y. Ding, L. O. Alimi, B. Moosa, G. Zhang, W. S. Baslyman, J. Sessler and N. M. Khashab, *Chem. Sci.*, 2021, **12**, 12286–12291.
- X. Liu, L. O. Alimi and N. M. Khashab, *Chem. Commun.*, 2022, **58**, 9369–9372.
- B. Moosa, L. O. Alimi, W. Lin, A. Fakim, P. M. Bhatt, M. Eddaoudi and N. M. Khashab, *Angew. Chem., Int. Ed.*, 2023, **62**, e202311555.
- D. Luo, J. Tian, J. L. Sessler and X. Chi, *J. Am. Chem. Soc.*, 2021, **143**, 18849–18853.
- Q. Li, K. Jie and F. Huang, *Angew. Chem., Int. Ed.*, 2020, **59**, 5355–5358.
- (a) M. Liu, R. Cen, J. Li, Q. Li, Z. Tao, X. Xiao and L. Isaacs, *Angew. Chem., Int. Ed.*, 2022, **61**, e202207209; (b) B. Li, Y. Wang, Y. Wang, Y. Liu, L. Wang, Z.-Y. Zhang and C. Li, *Chem. Commun.*, 2024, **60**, 6889–6892; (c) B. Hua, L. Shao, M. Li, H. Liang and F. Huang, *Acc. Chem. Res.*, 2022, **55**, 1025–1034; (d) J.-R. Wu, Z. Cai, G. Wu, D. Dai, Y.-Q. Liu and Y.-W. Yang, *J. Am. Chem. Soc.*, 2021, **143**, 20395–20402.
- L. O. Alimi, B. Moosa, W. Lin and N. M. Khashab, *ACS Mater. Lett.*, 2024, **6**, 1467–1473.
- Z. Cai, J. Du, T. Huang, Y. Ding and M. Wu, *CrystEngComm*, 2023, **25**, 5778–5781.
- S. La Cognata and V. Amendola, *Chem. Commun.*, 2023, **59**, 13668–13678.
- T. Tozawa, J. T. A. Jones, S. I. Swamy, S. Jiang, D. J. Adams, S. Shakespeare, R. Clowes, D. Bradshaw, T. Hasell, S. Y. Chong, C. Tang, S. Thompson, J. Parker, A. Trewin, J. Bacsá, A. M. Z. Slawin, A. Steiner and I. A. Cooper, *Nat. Mater.*, 2009, **8**, 973–978.
- B. Moosa, L. O. Alimi, A. Shkurenko, A. Fakim, P. M. Bhatt, G. Zhang, M. Eddaoudi and N. M. Khashab, *Angew. Chem., Int. Ed.*, 2020, **59**, 21367–21371.
- Y. Ding, L. O. Alimi, B. Moosa, C. Maaliki, J. Jacquemin, F. Huang and N. M. Khashab, *Chem. Sci.*, 2021, **12**, 5315–5318.
- L. O. Alimi, F. Fang, B. Moosa, Y. Ding and N. M. Khashab, *Angew. Chem., Int. Ed.*, 2022, **61**, e202212596 (*Angew. Chem.*, 2022, **134**, e202212596).
- A. C. Eaby, D. C. Myburgh, A. Kosimov, M. Kwit, C. Esterhuysen, A. M. Janiak and L. J. Barbour, *Nature*, 2023, **616**, 288–292.
- K. J. Hartlieb, J. M. Holcroft, P. Z. Moghadam, N. A. Vermeulen, M. M. Algaradh, M. S. Nassar, Y. Y. Botros, R. Q. Snurr and J. F. Stoddart, *J. Am. Chem. Soc.*, 2016, **138**, 2292–2301.

